

APPLICATION-ORIENTED CLASSIFICATION AND SEGMENTATION IN REMOTE SENSING: A SATELLITE IMAGE ANALYSIS APPROACH

Project Report submitted by

Adithi Ram
(4NM21AI002)

Aditi S Rao
(4NM21AI004)

Under the Guidance of

Mr. Mahesh B L
Assistant Professor Gd. II

*In partial fulfillment of the requirements for the award of
the Degree of*

Bachelor of Engineering in Artificial Intelligence and Machine Learning

from

Visvesvaraya Technological University, Belagavi

Department of Artificial Intelligence and Machine Learning
NMAM Institute of Technology, Nitte - 574110
(An Autonomous Institution affiliated to VTU, Belagavi)

NOVEMBER 2024

**DEPARTMENT OF ARTIFICIAL INTELLIGENCE AND MACHINE
LEARNING**

CERTIFICATE

Certified that the project work entitled

*"APPLICATION-ORIENTED CLASSIFICATION AND SEGMENTATION IN
REMOTE SENSING: A SATELLITE IMAGE ANALYSIS APPROACH"*

is a bonafide work carried out by

Adithi Ram (4NM21AI002)

Aditi S Rao (4NM21AI004)

in partial fulfilment of the requirements for the award of

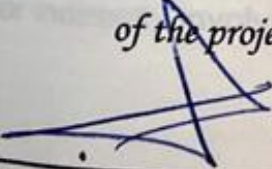
Bachelor of Engineering Degree in Artificial Intelligence and Machine Learning

prescribed by Visvesvaraya Technological University, Belagavi

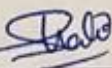
during the year 2024-2025.

*It is certified that all corrections/suggestions indicated for Internal Assessment have
been incorporated in the report deposited in the departmental library.*


*The project report has been approved as it satisfies the academic requirements in respect
of the project work prescribed for the Bachelor of Engineering Degree.*



Signature of the Guide



Signature of the HOD



Principal
N.M.A.M. Institute of Technology
Nitte, Karkala - 574 110

Semester End Viva Voce Examination

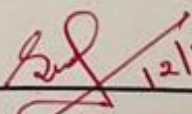
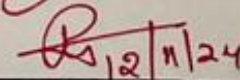
Name of the Examiners

Signature with Date

1. Sudesh Rao

2. Rakshitha



 12/11/24
 12/11/24

ACKNOWLEDGEMENT

The success and outcome of our project required the effort, assistance, and guidance of many people. We would like to acknowledge and thank all the parties involved in completing this project; without their support, we wouldn't have been able to make it successful.

First and foremost, we would like to thank our beloved Principal **Dr. Niranjan N. Chiplunkar**, and our college NMAM Institute of Technology for providing the resources and facilities required to execute the project.

Our sincere thanks to **Dr. Sharada Uday Shenoy**, Head of the Department, Department of Artificial Intelligence and Machine Learning, NMAMIT, Nitte, for her support and valuable input.

We would like to express our deepest gratitude to our project guide **Mr. Mahesh B L**, Assistant Professor Gd-II, Department of Artificial Intelligence and Machine Learning, NMAMIT, Nitte, for his constant encouragement, guidance, and suggestions for improvement throughout the duration of the project.

Our heartfelt thanks to the **Department of Artificial Intelligence and Machine Learning** staff members and our friends for their honest opinions and unconditional support.

We would like to take this opportunity to express our gratitude to everyone directly or indirectly involved in making this project successful.

Adithi Ram

Aditi S Rao

ABSTRACT

This project enhances the semantic segmentation of aerial imagery by classifying each pixel in satellite images into categories such as buildings, roads, vegetation, and water bodies. Our goal is to advance the accuracy of these classifications using state-of-the-art segmentation techniques. By employing U-Net and DeepLabV3+ architectures, we improve the precision and efficiency of identifying key features within complex land cover and urban environments. These encoder-decoder models excel in capturing intricate spatial patterns, enabling accurate extraction and classification of diverse terrain types. Building on this segmentation framework, we extend our approach to post-hurricane damage assessment, where a specialized neural network detects disaster-specific indicators, including structural destruction and scattered debris. Trained on large, heterogeneous datasets, this model provides rapid, resource-sensitive damage mapping that aids in immediate disaster management. Our findings reveal the potential of deep learning for precise, timely damage assessment, which can ultimately streamline recovery operations and support focused, efficient responses in post-disaster environments.

TABLE OF CONTENTS

Title page.....	(i)
Certificate.....	(ii)
Acknowledgement.....	(iii)
Abstract.....	(iv)
Table Of Contents.....	(v)
List of Figures.....	(vii)
List of Tables.....	(viii)
Chapter 1 Introduction	1-2
1.1 Overview	1
1.2 Problem Statement	1
1.3 Objectives	2
1.4 Motivation	2
Chapter 2 Literature Review	3-5
Chapter 3 System Requirements	6
3.1 Hardware Requirements	6
3.2 Software Requirements	6
3.3 Deep Learning Frameworks	6
Chapter 4 System Design	7
Chapter 5 Implementation	8-19
5.1 Implementation for Segmentation Model	8-11
5.1.1 Data Collection	8
5.1.2 Data Pre-processing	8
5.1.3 Model Development	9
5.1.4 Evaluation Metrics	10
5.1.5 System Architecture	11
5.2 Implementation for Classification Model	12-19

5.2.1 Data Collection	12
5.2.2 Exploratory Data Analysis	12-17
5.2.2.1 Visual Inspection	13
5.2.2.2 Trends by class – Mean Value	14
5.2.2.3 Trends by class – Standard Deviation	14
5.2.2.4 Contrast Mean Value	15
5.2.2.5 PCA + Eigen images	15
5.2.2.6 Geographic Distribution	17
5.2.3 Model Development	17
5.2.4 Evaluation Metrics	18
5.2.5 System Architecture	19
 Chapter 6 Results	 20-28
6.1 Results for U-Net Model	20
6.2 Implementation for DeepLab V3+ Model	22
6.3 Implementation for CNN Model	24
 Chapter 7 Conclusion and Future Work	 29
7.1 Conclusion	29
7.2 Future work	29
 Chapter 8 References	 30

LIST OF FIGURES

Figure 4.1 System Design.....	7
Figure 5.1 Workflow of the models.....	11
Figure 5.2 Sample images from the dataset.....	13
Figure 5.3 Mean value by class.....	14
Figure 5.4 Standard Deviation by class.....	14
Figure 5.5 Contrast between Mean Value	15
Figure 5.6 Eigen images of damage structures.....	16
Figure 5.7 Eigen images of no damage structures	16
Figure 5.8 Geographic Point Locations.....	17
Figure 5.9 System Architecture.....	19
Figure 6.1 Color Palette.....	20
Figure 6.2 Results of U-Net.....	21
Figure 6.3 Graphs of U-Net.....	21
Figure 6.4 Results of DeepLab V3+.....	22
Figure 6.5 Graphs of DeepLab V3+.....	23
Figure 6.6 Graphs of CNN model.....	24
Figure 6.7 Confusion matrix.....	24
Figure 6.8 False Negatives.....	25
Figure 6.9 False Positives.....	26
Figure 6.10 True Positives.....	27
Figure 6.11 True Negatives.....	28

LIST OF TABLES

Table 6.1 Model Performance of U-Net.....	22
Table 6.2 Model Performance of DeepLab V3+	23

CHAPTER 1

INTRODUCTION

1.1 OVERVIEW

Aerial imagery segmentation is essential in geospatial analysis, enabling pixel classification into categories like infrastructure, vegetation, water bodies, and open land. This detailed mapping is crucial for high-accuracy tasks in environmental conservation, urban growth analysis, and disaster response.

Recent advancements in deep learning, particularly with models like U-Net and DeepLabV3+, have significantly enhanced the accuracy of these classifications. U-Net's encoder-decoder structure captures spatial details for fine-grained segmentation, while DeepLabV3+ enhances contextual understanding through atrous convolutions and spatial pyramid pooling. This project aims to utilize both architectures for accurate segmentation of aerial imagery.

For post-hurricane damage assessment, an initial exploratory analysis of the dataset was conducted, followed by the implementation of a CNN model to identify structural damage, debris, and other disaster indicators. This approach allows for swift and precise evaluations of affected areas.

Ultimately the project enhances landscape analysis, supporting better decision-making in environmental sustainability, infrastructure planning, and disaster management. By generating quick damage assessment maps from a single aerial flyover, the model offers vital insights for post-disaster recovery, enabling agencies to rapidly assess impacts and allocate resources effectively.

1.2 PROBLEM STATEMENT

The goal of this project is to develop a robust and efficient semantic segmentation model for aerial imagery to accurately identify and label various features such as buildings, roads, vegetation, and water bodies. This task requires the model to handle the challenges posed by variations in scale, lighting conditions, and the

complexity of the scene. This model should leverage advanced techniques to handle the complexity and variability of aerial images, providing precise and reliable segmentation results suitable for applications in urban planning, agriculture and environmental monitoring. In future extensions, the model will also analyze post-hurricane damage to support disaster response efforts, enabling rapid assessment of affected areas and aiding in efficient resource allocation for recovery.

1.3 OBJECTIVES

- Design and implementation of robust deep learning model for multiclass semantic segmentation of high-resolution remote sensing images.
- To explore how segmentation techniques can enhance land cover classification for applications in environmental monitoring, urban planning and disaster response.
- To advance land management strategies by delivering enhanced techniques for analyzing and interpreting large-scale satellite imagery, emphasizing disaster management and land use assessment.

1.4 MOTIVATION

The motivation for segmenting satellite images for land use cover stems from the growing demand for accurate environmental data to support sustainable development and effective urban planning. By identifying and categorizing different land types, including urban areas and natural ecosystems, decision-makers can better optimize resource utilization and minimize ecological footprints. Furthermore, leveraging this segmentation for post-damage assessment significantly improves disaster response capabilities by facilitating the rapid identification of affected regions, enabling targeted resource allocation and streamlined recovery efforts. This holistic approach not only addresses urgent post-disaster needs but also fosters long-term resilience in the face of environmental uncertainties.

CHAPTER 2

LITERATURE REVIEW

[1] Bilel Benjdira et al. effectively addressed the issue of applying a model to new geographical areas not represented in its training dataset through the innovative use of a Generative Adversarial Network (GAN) architecture. Their approach consists of two distinct GAN networks: the first network converts a selected image from the target domain into a corresponding semantic label. The second network then transforms this generated semantic label into an image that aligns with the source domain while preserving the semantic integrity of the original target image. Utilizing the ISPRS semantic segmentation dataset, their methodology achieved a notable 24% improvement in accuracy when transitioning from the Potsdam domain to the Vaihingen domain.

[2] In 2023, Behera et al. proposed a unique multi-scale CNN architecture that incorporates superpixels to enhance classification accuracy in complex urban aerial images. Their innovative two-tier segmentation framework begins by generating superpixel images through linear iterative clustering, which captures essential contextual information. In the second tier, a multi-scale CNN analyzes these superpixels to extract invariant features for each pixel. Tested on the National Institute of Technology Rourkela (NITR) drone dataset and the urban drone dataset (UDD), their method demonstrated superior performance, achieving higher accuracy than existing approaches in challenging urban environments.

[3] A recent study by D. Jozi et al. introduced an innovative image-processing approach for assessing post-disaster building damage through UAV imagery. This method integrated texture-based features, like dissimilarity and homogeneity, with edge-based characteristics derived from Canny edge detection. Unique indices were proposed to capture structural irregularities by analyzing entropy and the uniformity of edge angle distributions. Using these features, a Naïve Bayesian classifier effectively distinguished damaged from undamaged buildings, achieving 89.3% accuracy on real-world disaster images. This research highlighted the

potential of UAV-based image analysis for fast, reliable damage assessment in post-disaster scenarios.

[4] Thakkar et al. proposes an innovative segmentation approach using a single-day image dataset from a village in Gujarat, obtained via Google Earth's Sentinel satellite imagery, to classify two key crops: wheat and Ricinus. The study evaluates various segmentation architectures, including machine learning (ML), deep learning (DL), and U-Net, optimizing performance through different learning rate strategies. The U-Net architecture achieved a validation accuracy of 94.6% at 500 m altitude, while the ResUNet with a cyclic learning rate for 1000 m altitude images surpassed traditional methods, reaching 98.5% accuracy. These findings highlight the superior performance of U-Net and its variants with cyclic learning rates over conventional ML and DL techniques in agricultural segmentation tasks.

[5] In 2021, Zhang et al. proposed an innovative atrous spatial pyramid pooling U-Net (ASPP-U-Net) to enhance the speed and accuracy of land-cover classification for medium-resolution remote-sensing images. This advanced model is specifically designed to leverage the unique characteristics of medium-resolution imagery, outperforming conventional techniques such as SVM, patch-based CNN, and traditional U-Net in terms of both classification precision and inference efficiency. Their results suggest that ASPP-U-Net is a highly effective method for mapping land cover in medium-resolution images. However, the authors note that the potential for further improvements in classification accuracy may be hindered by the presence of inaccurately labelled reference data.

[6] The article by C. Kyrkou and T. Theocharides, explored improvements in aerial image classification for emergency response using UAVs. It introduced a specialized Aerial Image Database for Emergency Response applications and performed a detailed comparison of existing methods. From this analysis, a new lightweight convolutional neural network called EmergencyNet was developed, which used atrous convolutions to efficiently process multi-resolution features. This architecture was designed to run effectively on low-power embedded platforms, achieving up to 20 times better performance than existing models. Importantly, it

maintained minimal memory use and had less than 1% accuracy loss compared to state-of-the-art methods.

[7] This study presented a machine-learning approach for autonomous drones to identify and prioritize flood-affected areas using image classification. The system combined Inception v3 and DenseNet CNNs with a sorting algorithm to guide relief efforts, prioritizing the most affected areas first. Inception v3 performed better, achieving 83% accuracy compared to DenseNet's 81% on a custom flood severity dataset. This approach demonstrated CNNs' potential in supporting autonomous decision-making for robotic disaster response.

CHAPTER 3

SYSTEM REQUIREMENTS

3.1 HARDWARE REQUIREMENTS

- **System type:** 32/64-bit operating system
- **Operating System:** Windows 10 and above
- **RAM:** 8 GB

3.2 SOFTWARE REQUIREMENTS

- **Python 3:** Core programming language used for implementing the machine learning model, data processing and for analyzing the results.
- **Anaconda:** Anaconda is used as the Python distribution for managing packages, dependencies, and environments.
- **Notebook:** Jupyter Notebook for interactive running and markdown, popular for data analysis and scientific computing.

3.3 DEEP LEARNING FRAMEWORKS

- **NumPy** for vectorized implementation and fast arrays
- **Pandas** for dealing with tabular and high dimensional data
- **Matplotlib** for plotting and visualizations
- **OpenCV** for image manipulations
- **Tensorflow** for Deep Learning
- **Keras** models for Computer Vision
- **Patchify** for creating patches of the images by cropping to re-patching instead of resizing all the different sizes of the images

CHAPTER 4

SYSTEM DESIGN

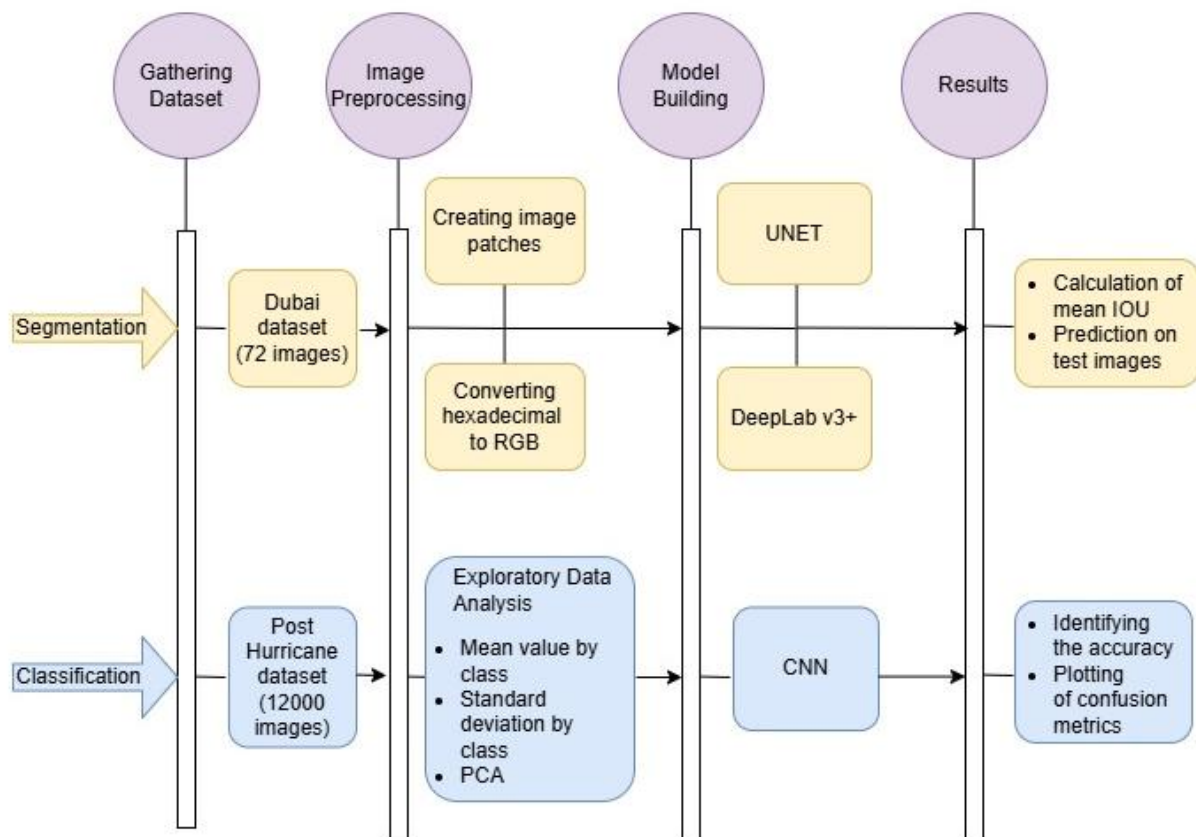


Figure 4.1 illustrates the sequence diagram of the system

Figure 4.1 illustrates the process of image segmentation, starting with the Dubai dataset as input. The images are prepared by converting to RGB and dividing them into smaller patches for easier processing. Two powerful models, UNET and DeepLab V3+ are then employed to identify and separate objects within the images. The models' performance is evaluated using the mean Intersection over Union (IoU) score, which measures segmentation accuracy.

The next task focuses on classifying images from the post-hurricane dataset into predefined classes. This involves preprocessing the images, conducting exploratory data analysis to understand data distribution, and training a Convolutional Neural Network model for classification. The model's effectiveness is assessed using accuracy and confusion matrices.

CHAPTER 5

IMPLEMENTATION

5.1 IMPLEMENTATION FOR SEGMENTATION MODEL

5.1.1 Data Collection

This study utilizes a satellite imagery dataset of Dubai, captured by MBRSC satellites and segmented at a pixel level into six classes. The dataset was meticulously annotated by trainees from the Roia Foundation in Syria and is publicly available under the CC0 1.0 license, contributed by Humans in the Loop. It includes eight large imaging tiles, each subdivided into nine uniform patches, amounting to a total 72 unique images.

The classes are:

1. Building : #3C1098
2. Land : #8429F6
3. Road : #6EC1E4
4. Vegetation : #FEDD3A
5. Water : #E2A929
6. Unlabelled : #9B9B9B

5.1.2 Data Preprocessing

Two preprocessing steps are used :

1. Creating image patches using Patchify

Patchify is a technique that divides large images into smaller patches or tiles of a defined size. Using patchify, patches are created for the images and masks. For example, Tile 1 measures 797 x 644 and yields six patches of size 768 x 512; Tile 2, measuring 509 x 544, produces two patches of size 512 x 256 and so on.

- **Tile 1:** 797 x 644 --> 768 x 512 --> 6
- **Tile 2:** 509 x 544 --> 512 x 256 --> 2

- **Tile 3:** 682 x 658 --> 512 x 512 --> 4
- **Tile 4:** 1099 x 846 --> 1024 x 768 --> 12
- **Tile 5:** 1126 x 1058 --> 1024 x 1024 --> 16
- **Tile 6:** 859 x 838 --> 768 x 768 --> 9
- **Tile 7:** 1817 x 2061 --> 1792 x 2048 --> 56
- **Tile 8:** 2149 x 1479 --> 1280 x 2048 --> 40

In total, there are nine images in each folder, yielding 145 patches per image, culminating in a total of 1,305 patches, all sized at 256 x 256.

2. Hexadecimal to RGB

To convert a hexadecimal color code to RGB, the process involves interpreting each pair of hexadecimal digits. The range of digits is represented as 0-9 for values 0-9 and A-F for values 10-15. For example, given the hex color code #3C1098, the conversion process is as follows: the first pair, "3C," is calculated by multiplying 3 by 16 and adding 12 (C), resulting in a decimal value of 60. The second pair, "10," is computed as 1 multiplied by 16 plus 0, yielding a decimal value of 16. Lastly, for the pair "98," the calculation involves multiplying 9 by 16 and adding 8, which gives a decimal value of 152. Thus, the RGB values corresponding to the hex code #3C1098 are R = 60, G = 16, and B = 152.

5.1.3 Model Development

After data preprocessing, the U-Net and DeepLabv3+ models are constructed using multiple layers of neural networks for both the encoder and decoder structures. The models are subsequently trained and tested on satellite imagery from the dataset.

Standard U-NET

U-Net stands out as a prominent architecture for image segmentation, introduced in 2015 as a groundbreaking advancement in the processing of biomedical images,

and developed from the principles of traditional convolutional neural networks. This innovative architecture is distinguished by its unique U-shaped configuration, which incorporates an encoder-decoder framework. The encoder adeptly captures intricate image features through successive convolutions and down-sampling, while the decoder meticulously reconstructs these features, up-sampling them back to the original input dimensions. This process allows for the accurate localization and classification of each pixel into designated semantic categories. The U shape is a defining characteristic, formed by the connections between convolutional blocks at the base of the network, which not only facilitates a seamless transition from feature extraction to reconstruction but also enhances the model's ability to preserve vital spatial information throughout the segmentation journey.

DEEPLAB V3+

DeepLabv3+ is the latest advancement in the esteemed DeepLab series of deep learning architectures for semantic image segmentation, originally open-sourced by Google Inc. in 2016. This architecture retains the encoder-decoder framework while introducing the innovative Atrous Spatial Pyramid Pooling (ASPP) strategy. ASPP applies parallel dilated convolutions at various rates to the input feature map, enabling the model to seamlessly integrate features across multiple scales, which is essential for accurately segmenting objects of differing sizes within a single image. Furthermore, DeepLabv3+ employs Dilated Convolutions, which enhance conventional convolutions by inserting gaps within the kernel elements, dictated by a parameter known as the dilation rate. This unique approach allows for a wider coverage of the input image without the need for pooling, thereby enriching the model's ability to gather comprehensive contextual information with each convolutional operation.

5.1.4 Evaluation Metrics

For performance evaluation, we utilized accuracy and the Jaccard Coefficient (also known as Intersection over Union, IoU) as key metrics for analyzing the results of the project.

The Jaccard Coefficient also referred to as Intersection over Union (IoU), is a widely used metric to assess the similarity between two sets, particularly in image segmentation tasks where it quantifies how well the predicted segmentation aligns with the actual ground truth. Its formula is the ratio of the intersection area of the predicted set (P) and the ground truth set (G) to their union:

$$\text{IoU} = \frac{|P \cap G|}{|P \cup G|}$$

In this calculation, $|P \cap G|$ represents the shared pixels between the predicted and actual regions, while $|P \cup G|$ accounts for the total area covered by both. The IoU score ranges from 0 to 1, where 0 indicates no overlap, and 1 indicates a perfect match. This metric provides a more nuanced evaluation by considering both the correctly predicted areas and the erroneous regions, offering a clearer view of segmentation performance.

Both the models gave an accuracy of 86% on the test data and the mean IoU obtained was 60% which means that, on average, 60% of the pixels in the predicted segmentation overlap with the pixels in the ground truth segmentation for each class. Higher IoU values indicate better performance, with 100% being a perfect overlap.

5.1.5 System Architecture

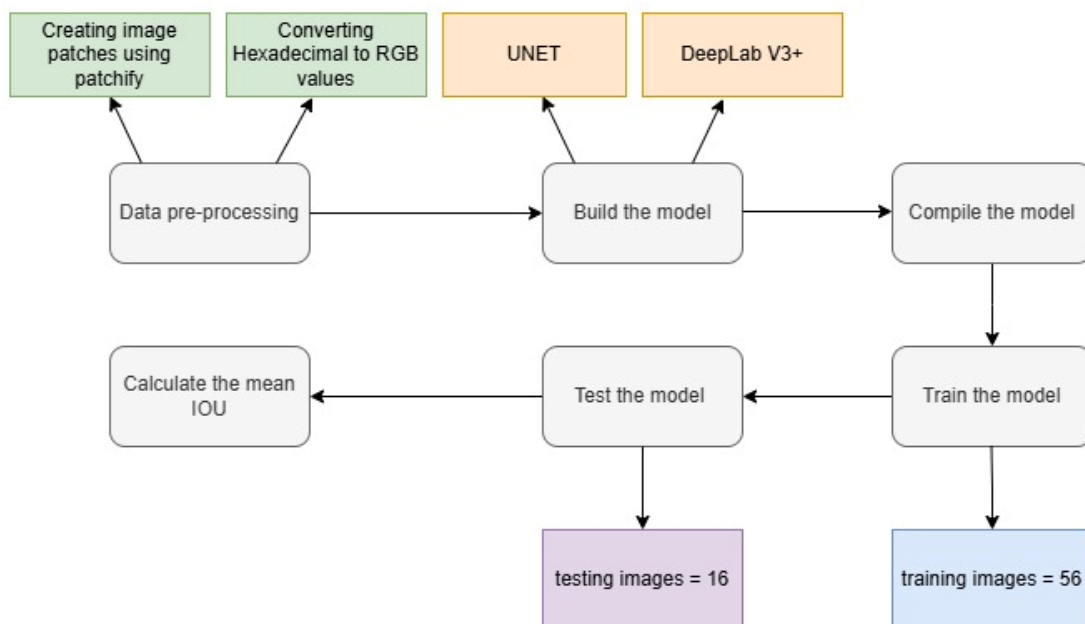


Figure 5.1 illustrates the workflow of the two models

The Figure 5.1 illustrates the preprocessing of data from the Dubai dataset which involves converting hexadecimal values to RGB and creating image patches. Following this, model building and training are performed using architectures like UNET and DeepLab V3+. The model is compiled and trained on a dataset of 504 images, which includes 56 original training images and 448 augmented ones. Finally, the trained model is evaluated on a separate test set of 16 images. The Intersection over Union (IoU) metric is used to assess the model's performance in accurately segmenting objects within the images.

5.2 IMPLEMENTATION FOR CLASSIFICATION MODEL

5.2.1 Data Collection

This project used a labelled dataset from Quoc Dung Cao and Youngjun Choe at the University of Washington's Disaster Data Science Lab. The dataset contains images of buildings taken from aerial photos after Hurricane Harvey in Houston in August 2017 and nearby areas, with labels showing whether each building was damaged.

Images in the dataset are organized into training, validation, and test sets. The training dataset includes 10,000 images (5,000 no damage, 5,000 with damage) and the validation and test sets each include 2,000 images (1,000 no damage, 1,000 with damage). The filename for each image includes the latitude and longitude coordinates which can be used to plot the locations of the structures in relation to each other.

5.2.2 Exploratory Data Analysis

Before training our neural network, we conducted a thorough data exploration to identify patterns in the dataset. We began by plotting example images from each class to gain a shared visual understanding. Next, we analyzed trends by creating summary images to visualize metrics like the mean, standard deviation, and contrast between the classes. Then, we applied principal component analysis (PCA) to highlight common features in the images. Finally, we mapped the

geographic locations of the images to understand the spatial distribution of structures across the dataset.

5.2.2.1 Visual Inspection

The images are in RGB colour format. The figure below shows a comparison between three randomly selected images of damaged areas and three randomly selected images of undamaged areas. Observing these and other examples revealed some emerging patterns.

- Many images show floodwaters surrounding the structures, leading to differences in ground texture and colour, although this is not true for all cases.
- Some damaged-area images feature small objects scattered across the ground; however, this pattern is also present in several undamaged-area images.
- Images of undamaged structures are more likely to show visible ground or pools of blueish water, free from floodwaters.
- In many cases, it's challenging for the human eye to clearly distinguish between images showing damage and those without.



Figure 5.2 sample images from the dataset

5.2.2.2 Trends by class – Mean Value

The figure 5.3 depicts each pixel's mean value across all images by class. For both damage and no damage images, we see that a structure tends to be located within the center of the image. For damage images, the pixel values around the structure tend to be lower in value than around the no damage images. Perhaps this is because damage images tend to have flood waters around the structures, which are a different color than unflooded ground.

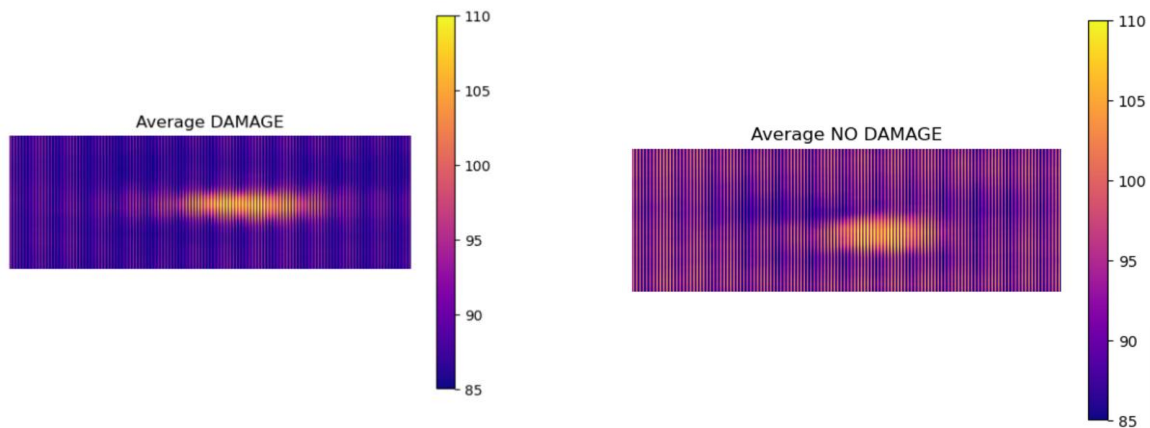


Figure 5.3 represents mean value class of damage and no damage images

5.2.2.3 Trends by class – Standard Deviation

The figure 5.4 are similar to those above but instead of depicting the mean pixel value they depict the standard deviation for each pixel by class. Standard deviation around the edges of the image appears to be (slightly) greater for the no damage images. Perhaps this is because visible ground around the structures creates more variation between images in that class.

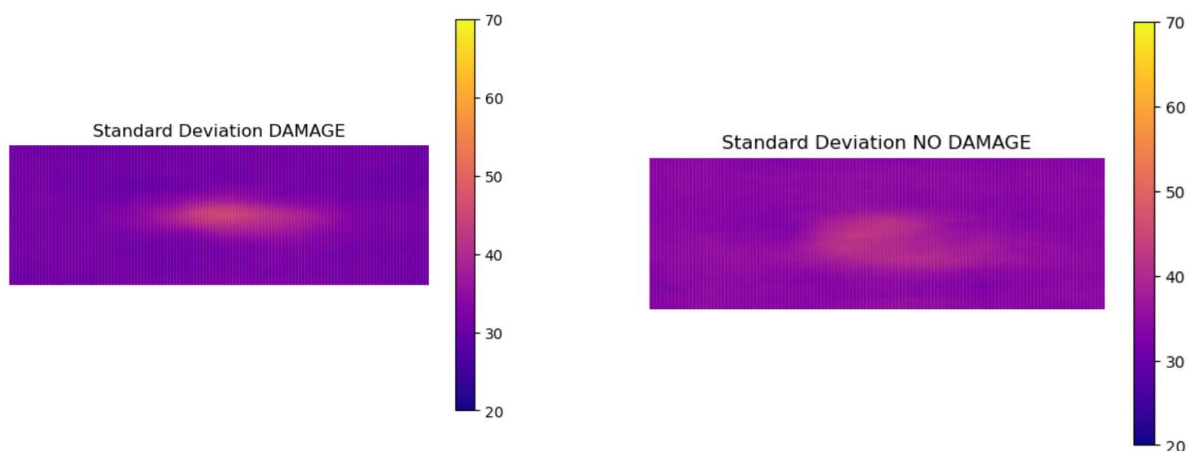


Figure 5.4 represents standard deviation by class of damage and no damage images

5.2.2.4 Contrast Between Mean Value by Class

In the figure 5.5, pixel values are the difference between the mean images for the two classes (damage and no damage) displayed above. Dark blue and dark red pixels are where there is the greatest difference between mean values across the two classes and white is where there is the least. The white pixels appear to form the outline of a structure - this is expected since all images of both classes have a structure in the center of the image. The difference values are higher in the center and edges (area surrounding the structure)

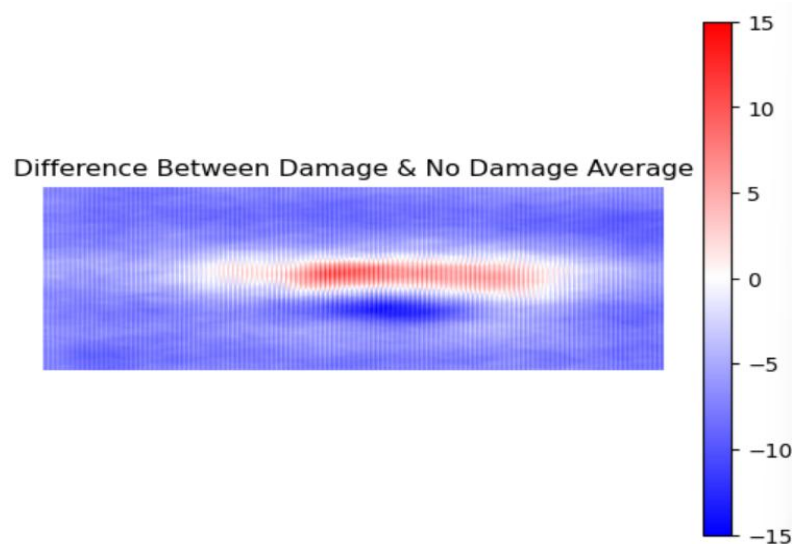


Figure 5.5 represents contrast between mean value by class of damage and no damage images

5.2.2.5 PCA + Eigen images

We used PCA to create eigen images for two image classes to capture key patterns within each image. The eigen images are not easily recognizable to the human eye, unlike eigen images based on faces or other images with more regular repeating features. The images below are hints of basic geometric shapes with right angles, and only highlight the primary patterns.

For images depicting structures with damage, 22 principal components explained 70% of the variation:

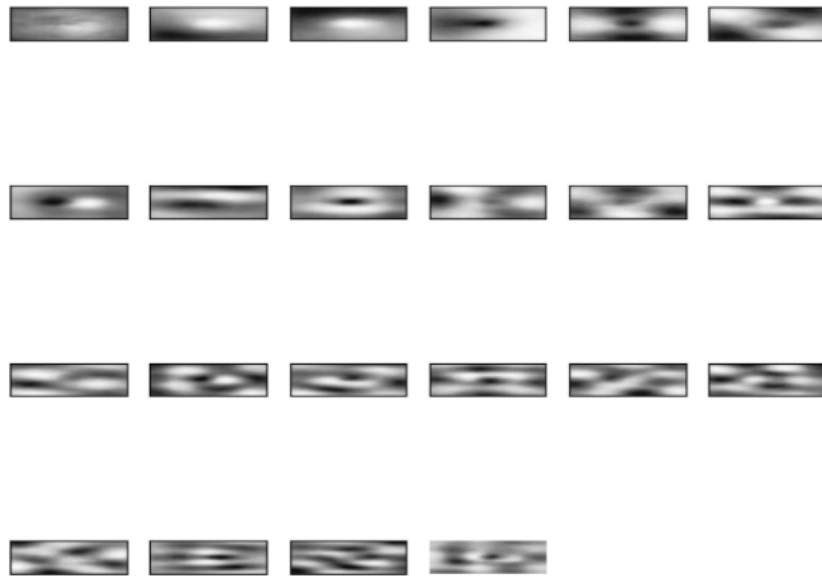


Figure 5.6 eigen images depicting structures with damage

For images depicting structures with no damage, 61 principal components explained 70% of the variation:



Figure 5.7 eigen images depicting structures with no damage

5.2.2.6 Geographic Distribution

Finally we investigated the geographic distribution of the training data by class. This is possible because the GPS coordinates are contained in the filename for each image file. The figure below depicts the locations of each image in the training dataset and whether it is damaged or not damaged

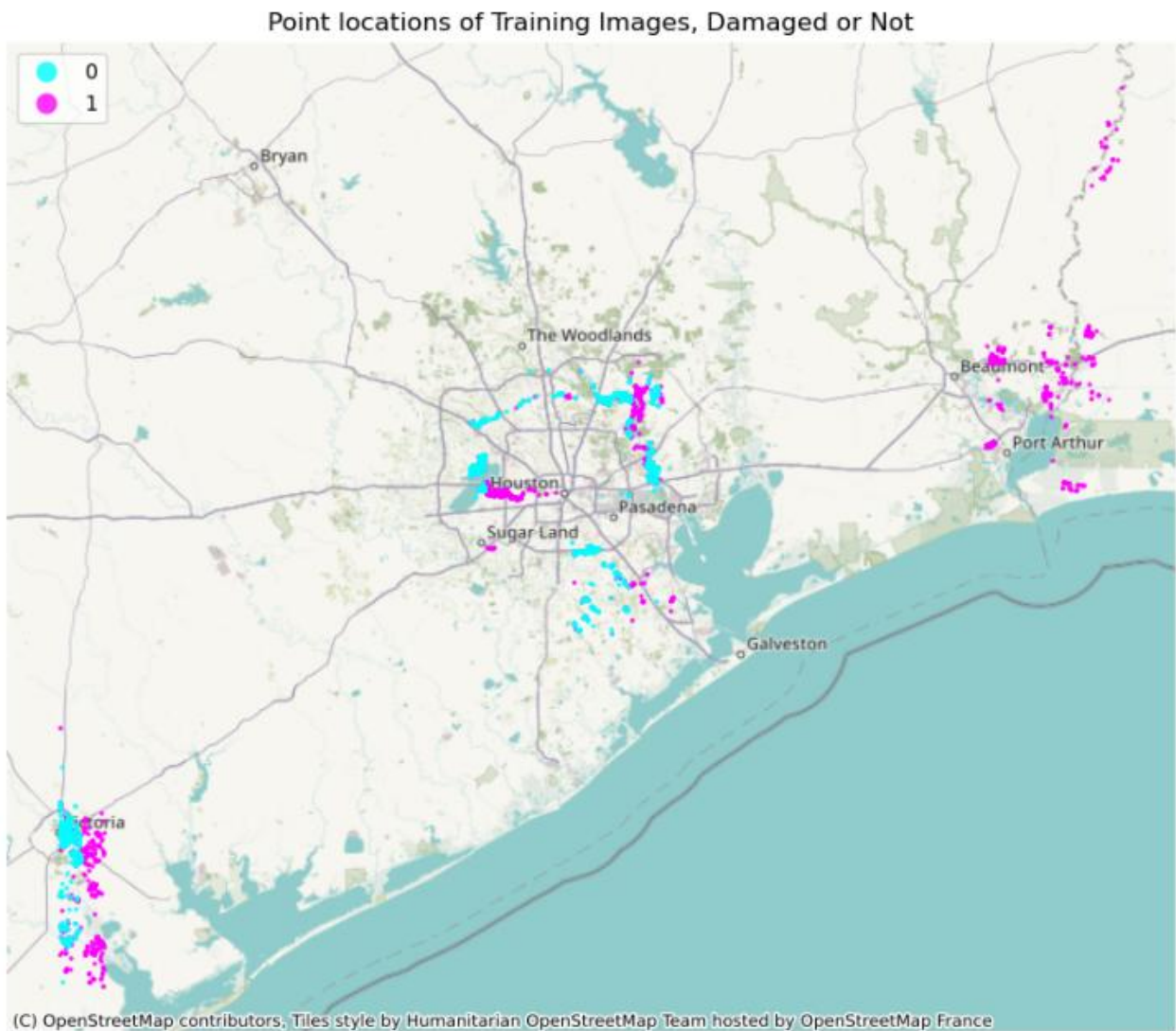


Figure 5.8 represents point locations of training images
1: damaged ; 0: no damage

5.2.3 Model Development

To build the model , we have used a simple convolution neural network. The model is trained and tested on the dataset.

Convolution Neural Network

A Convolutional Neural Network (CNN) is a type of deep learning model designed for processing visual data, like images. The model begins with an input layer, followed by three convolutional layers with max-pooling, batch normalization, and ReLU activation functions to learn spatial features in the input images. After flattening these feature maps, the model includes dense layers with dropout to reduce overfitting and improve generalization. The final dense layer has a softmax activation for classification, outputting probabilities across the classes. The Adam optimizer with a custom learning rate is used for optimization, and early stopping with model check pointing ensures that the best-performing model is saved based on validation accuracy, avoiding overfitting by stopping training when improvements slow down.

5.2.4 Evaluation Metrics

The final model was then evaluated on test data. The metrics used were accuracy and confusion matrix.

Accuracy metrics evaluate model performance in classification tasks. It measures the proportion of correct predictions made by a model out of the total predictions. It's calculated as the ratio of correctly classified instances (both true positives and true negatives) to all instances, including false positives and false negatives.

A confusion matrix is an essential tool for evaluating classification model performance by summarizing predicted versus actual labels. It consists of four components for binary classification: True Positive, True Negative, False Positive, and False Negative. The diagonal cells indicate correct predictions, while the off-diagonal cells represent errors. Various performance metrics, such as accuracy, precision, recall, and the F1 score, can be derived from the matrix. It helps identify types of errors, guiding improvements and providing insights, especially in imbalanced datasets where accuracy alone can be misleading.

Our model gave an accuracy of 97% on the test data.

5.2.5 System Architecture

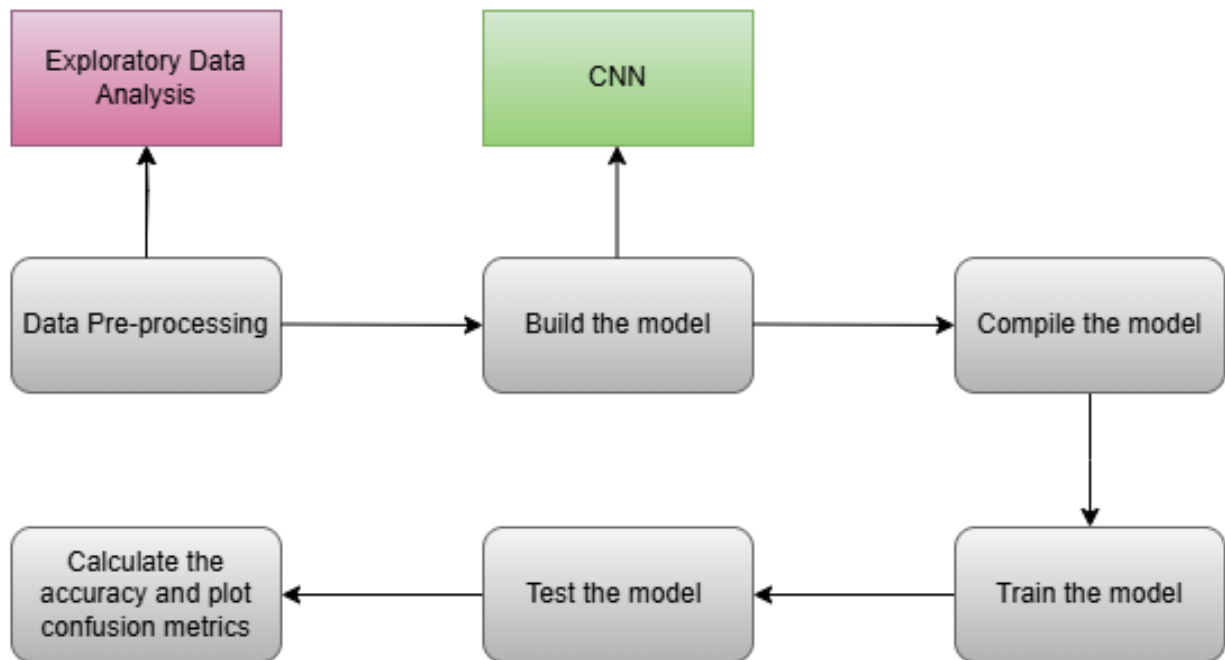


Figure 5.9 represents the workflow of the classification model

This Figure 5.9 outlines the process of building and evaluating a Convolutional Neural Network (CNN) for image classification. The process begins with Exploratory Data Analysis to understand the dataset, followed by data preprocessing to prepare the data for modeling. The CNN model is then built and compiled to specify the optimizer, loss function, and evaluation metrics. The model is trained on the dataset and subsequently tested to assess its performance. Finally, the accuracy and confusion matrix are calculated and plotted to evaluate the model's effectiveness in classification. This workflow ensures a structured approach to training and assessing the CNN model.

CHAPTER 6

RESULTS AND DISCUSSIONS

The Figure 6.1 shows a color palette with six colors and their corresponding RGB values. Each color is named with labels like "Building," "Land," "Road," etc., suggesting that this palette might be used to visually represent different land cover types or objects in a geographic dataset. This could be useful for creating color-coded maps or visualizations in fields like remote sensing, GIS, or urban planning.

Name	R	G	B	Color
Building	60	16	152	
Land	132	41	246	
Road	110	193	228	
Vegetation	254	221	58	
Water	226	169	41	
Unlabeled	155	155	155	

Figure 6.1 represents the color palette for geographic data.

6.1 RESULTS OBTAINED FOR UNET MODEL

The Figure 6.2 illustrates the outcomes of an image segmentation task, displaying the original image alongside its corresponding ground truth segmentation and the

segmentation predicted by the U-Net model. The objective is to evaluate the model's accuracy in segmenting various objects within the image, including buildings, roads, and vegetation. A close alignment between the predicted segmentation and the ground truth indicates that the model has successfully learned to identify and segment the different objects within the image.

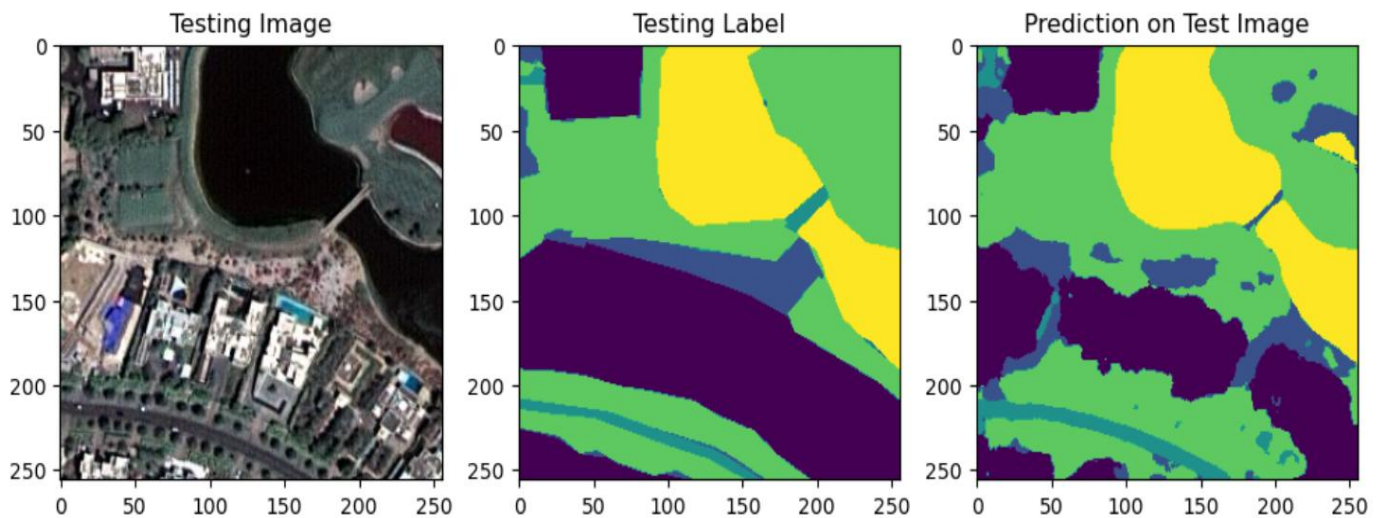


Figure 6.2 illustrates results of U-Net segmentation model

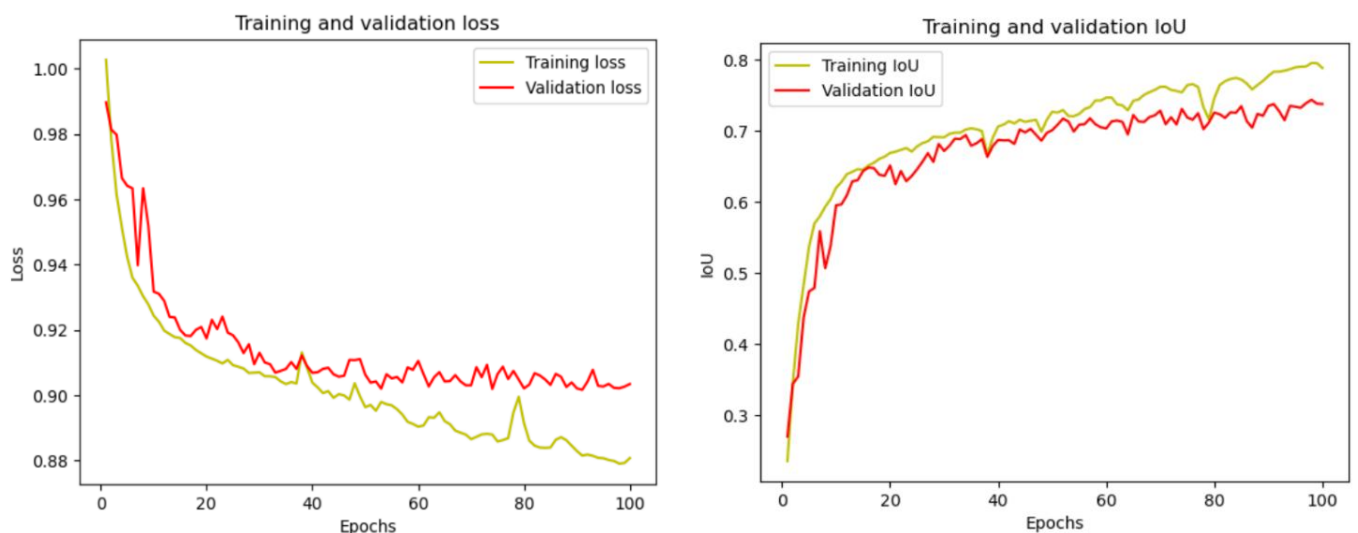


Figure 6.3 illustrates the graphs for IoU and loss metrics of U-Net segmentation model

The Table 6.1 shows the training and validation performance of the U-Net model over 100 epochs. As the model trains, its loss decreases, and its accuracy increases on both the training and validation datasets.

Epochs	Loss	Accuracy	Val_loss	Val_accuracy
5	0.9453	0.7561	0.9641	0.6880
25	0.9092	0.8462	0.9183	0.8182
50	0.8970	0.8685	0.9063	0.8525
75	0.8870	0.8902	0.9065	0.8592
100	0.8827	0.9026	0.9034	0.8686

Table 6.1 illustrates model performance over time

6.2 RESULTS OBTAINED FOR DEEPLAB V3+ MODEL

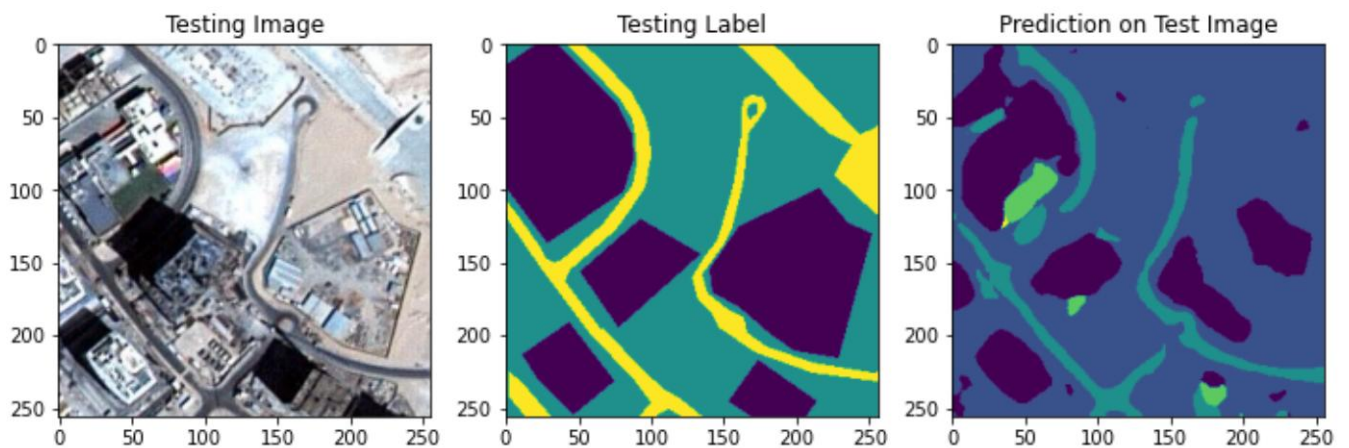


Figure 6.4 illustrates results of DeepLab V3+ segmentation model

The Figure 6.4 illustrates the outcomes of an image segmentation task, displaying the original image alongside its corresponding ground truth segmentation and the segmentation predicted by the DeepLab V3+ model.

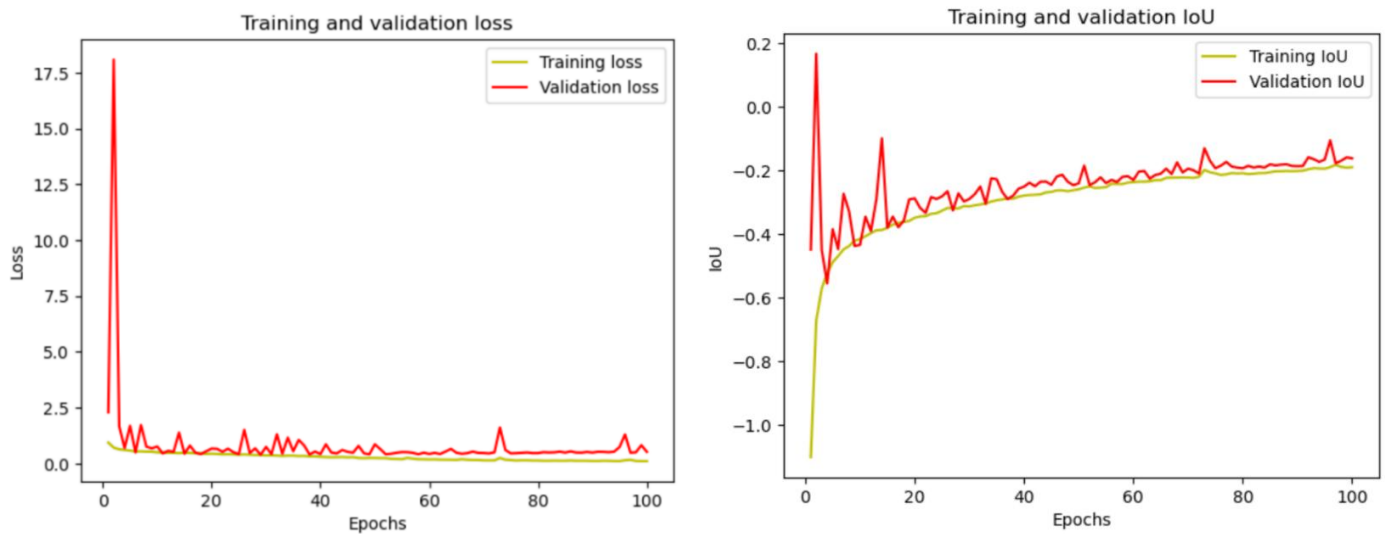


Figure 6.5 illustrates the graphs for IoU and loss metrics of DeepLab V3+ model

Epochs	Loss	Accuracy	Val_loss	Val_accuracy
5	0.5618	0.8146	1.6883	0.2813
25	0.3993	0.8588	0.4133	0.8580
50	0.2213	0.9198	0.8549	0.6801
75	0.1683	0.9364	0.4506	0.8688
100	0.1040	0.9593	0.5218	0.8638

Table 6.2 illustrates model performance over time

The Table 6.2 shows the training and validation performance of the U-Net model over 100 epochs. As the model trains, its loss decreases, and its accuracy increases on both the training and validation datasets.

6.3 RESULTS OBTAINED FOR CONVOLUTION NEURAL NETWORK MODEL

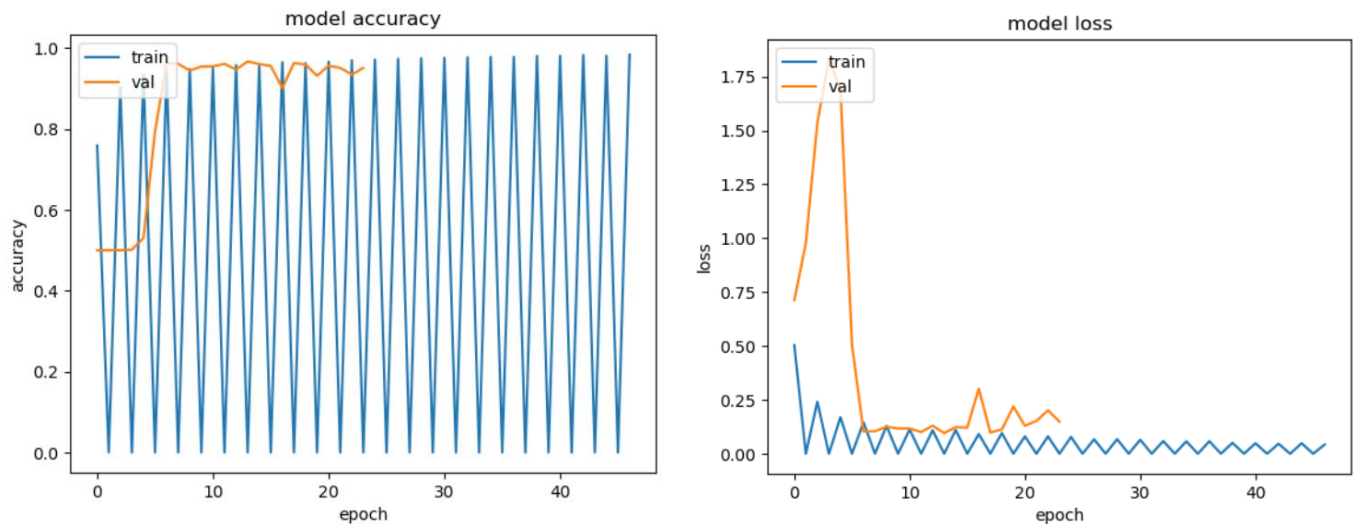


Figure 6.6 illustrates the graphs for accuracy and loss metrics of the CNN model

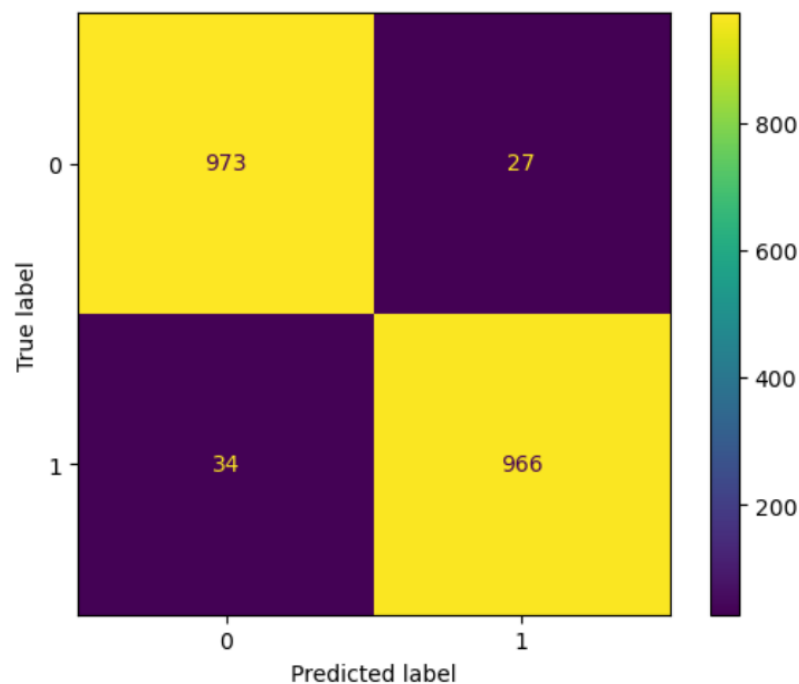


Figure 6.7 represents the confusion matrix

This confusion matrix provides an overview of the model's performance in classifying images as either "damage" (1) or "no damage" (0). The model correctly identified "no damage" in 973 cases and "damage" in 966 cases, showing a strong ability to make accurate predictions. However, there were some misclassifications:

27 cases were incorrectly predicted as "damage" when there was actually "no damage" (false positives), and 34 cases were incorrectly predicted as "no damage" when there was actually "damage" (false negatives).

Examining the misclassified images reveals some insights about the model:

False negatives (34 total) appear to be mostly large or non-residential structures, have a lot of variation in the ground surface, and/or no obvious flood water



Figure 6.8 represents false negative images

False Positives (27 total) tend to have surfaces that are mistaken for flood waters or junk around them that is mistaken for damage. False positives also tend to be rural structures:



Figure 6.9 represents false positive images

Examining correctly classified images :



Figure 6.10 represents true positive images

Figure 6.10 tend to have obvious flood water, or scattered materials. Some of these aren't obvious to the human eye.



Figure 6.11 represents true negative images

Figure 6.11 tend to be obviously not flooded (visible ground) - but there are also examples that do have water or surfaces that look like flood water to the human eye.

CHAPTER 7

CONCLUSION AND FUTURE WORK

7.1 CONCLUSION

In conclusion, our project highlights the importance of segmenting satellite imagery for both land cover analysis and disaster assessment. Through precise classification of land cover types, we provided valuable insights that empower stakeholders to make informed decisions on sustainable development and resource management, fostering a more balanced interaction with the environment. Furthermore, applying our segmentation techniques to disaster assessment facilitated the rapid identification of affected areas, ensuring efficient resource allocation and effective emergency response. This integrated approach not only addresses the urgent needs following a disaster but also contributes to building long-term resilience and sustainable practices, positioning our work as a vital tool for navigating future environmental challenges.

7.2 FUTURE WORK

Future work in segmenting satellite imagery for land cover and disaster assessment could involve integrating data from sources like LiDAR and ground surveys to enhance accuracy. Developing real-time processing algorithms would allow for rapid insights during disasters, enabling quicker responses and more effective resource allocation. Additionally, improving deep learning models could further refine classification results. Implementing automated change detection systems would facilitate continuous monitoring of land cover, aiding in the early identification of disaster-prone areas. Creating user-friendly tools will help urban planners and disaster responders make better use of these insights. Finally, conducting field validation studies will ensure the reliability of results, while long-term monitoring of climate change impacts can inform policy decisions.

CHAPTER 8

REFERENCES

1. B. Benjdira, A. Ammar, A. Koubaa, and K. Ouni, "Data-Efficient Domain Adaptation for Semantic Segmentation of Aerial Imagery Using Generative Adversarial Networks," *Appl. Sci.*, vol. 10, no. 3, p. 1092, 2020, doi: 10.3390/app10031092.
2. T. K. Behera, S. Bakshi, M. Nappi and P. K. Sa, "Superpixel-Based Multiscale CNN Approach Toward Multiclass Object Segmentation From UAV-Captured Aerial Images," in *IEEE Journal of Selected Topics in Applied Earth Observations and Remote Sensing*, vol. 16, pp. 1771-1784, 2023, doi: 10.1109/JSTARS.2023.3239119.
3. D. Jozi, N. Shirzad-Ghaleroudkhani, G. Luhadia, S. Abtahi, and M. Gül, "Rapid post-disaster assessment of residential buildings using Unmanned Aerial Vehicles," **International Journal of Disaster Risk Reduction**, vol. 111, p. 104707, 2024, doi: 10.1016/j.ijdr.2024.104707.
4. M. Thakkar, R. Vanzara, and A. Patel, "Semantic segmentation approaches for crop classification with multi-altitude Google Earth imagery", *J Integr Sci Technol*, vol. 12, no. 6, p. 832, Jun. 2024, doi: 10.62110/sciencein.jist.2024.v12.832.
5. W. Zhang, P. Tang and L. Zhao, "Fast and accurate land-cover classification on medium-resolution remote-sensing images using segmentation models", *Int. J. Remote Sens.*, vol. 42, no. 9, pp. 3277-3301, May 2021.
6. C. Kyrkou and T. Theocharides, "EmergencyNet: Efficient Aerial Image Classification for Drone-Based Emergency Monitoring Using Atrous Convolutional Feature Fusion," in *IEEE Journal of Selected Topics in Applied Earth Observations and Remote Sensing*, vol. 13, pp. 1687-1699, 2020, doi: 10.1109/JSTARS.2020.2969809.

7. Md A. Islam, S. I. Rashid, N. U. I. Hossain, R. Fleming, and A. Sokolov, "An integrated convolutional neural network and sorting algorithm for image classification for efficient flood disaster management," *Decision Analytics Journal*, vol. 7, p. 100225, 2023. doi: 10.1016/j.dajour.2023.100225.
8. I. Ahmed, M. Ahmad, G. Jeon and A. Chehri, "An Internet of Things and AI-Powered Framework for Long-Term Flood Risk Evaluation," in *IEEE Internet of Things Journal*, vol. 11, no. 3, pp. 3812-3819, 1 Feb.1, 2024, doi: 10.1109/JIOT.2023.3308564.
9. A. A. Deshmukh, S. D. B. Sonar, R. V. Ingole, R. Agrawal, C. Dhule and N. C. Morris, "Satellite Image Segmentation for Forest Fire Risk Detection using Gaussian Mixture Models," *2023 2nd International Conference on Applied Artificial Intelligence and Computing (ICAAIC)*, Salem, India, 2023, pp. 806-811, doi: 10.1109/ICAAIC56838.2023.10140399.
10. L. He, J. Shan and D. Aliaga, "Generative Building Feature Estimation From Satellite Images," in *IEEE Transactions on Geoscience and Remote Sensing*, vol. 61, pp. 1-13, 2023, Art no. 4700613, doi: 10.1109/TGRS.2023.3242284.